

Electronic Supplementary Information

Synthesis of donor-substituted *meso*-phenyl and *meso*-ethynylphenyl BODIPYs with broad absorption

Katja Gräf, Thomas Körzdörfer, Stephan Kümmel, Mukundan Thelakkat

- 1 Mechanism of the Knoevenagel-type Condensation of MeOTPA-aldehyde with BODIPY
- 2 NMR Spectra
- 3 Determination of the double bond geometry of **12**
- 4 Additional UV/vis Spectra
- 5 Cyclic Voltammetry Data

1. Mechanism of the Knoevenagel-type Condensation of MeOTPA-aldehyde with BODIPY

The common synthetic strategy to extend the π -conjugation of BODIPYs is the attachment of aromatic donor groups at 3 and 5 positions using Knoevenagel-type condensations. In particular, an aromatic aldehyde is reacted with the methyl groups in the positions 3 and 5 of the BODIPY creating a vinylic bond. Although, this is a typical modification route, its mechanism has not yet been studied. It is only considered as Knoevenagel-type condensation involving a deprotonation of the acidic methyl groups in position 3 and 5 as they can be deprotonated under mild conditions and will readily react with electron rich aromatic aldehydes. To gain a better understanding of this condensation reaction on BODIPYs in general, we investigated the mechanism of this reaction.

For Knoevenagel-type condensations two mechanisms are proposed: the Hann-Lapworth¹ (Fig. S1) and the organocatalytic mechanism² (Fig. S2). With the used educts (3,5-dimethyl BODIPY, aromatic donor aldehyde and secondary amine), both reaction mechanisms are conceivable for the attachment of donors to the BODIPY scaffold. The Hann-Lapworth mechanism includes the deprotonation of the reactive methyl/methylene compound by an amine base.¹ The resonance stabilized carbanion is able to attack the electropositive carbon atom of the aldehyde in a nucleophilic reaction (Fig. S1). Thus, a new C-C bond with an alkoxide functionality will be formed which has to be protonated either by the protonated base or by the solvent. Hence, protic solvents are advantageous for this kind of reaction. In the last step, the β -hydroxy compound undergoes dehydration to afford the unsaturated product. The mechanism can be proven by the isolation of the β -hydroxy intermediate. However, in reactions between 3,5-dimethyl BODIPYs and aromatic aldehydes in presence of the secondary base piperidine we could not find any evidence for the formation of such a β -hydroxy intermediate. Instead, an aminal (Fig. S2, product **B**) was isolated. (See Fig. S3 for the NMR spectra of the aminal). The identification and isolation of this aminal proves that the Hann-Lapworth mechanism is not valid in this case.

¹ A. C. O. Hann and A. Lapworth, *J. Chem. Soc., Trans.*, 1904, **85**, 46.

² S. Bednarz and D. Bogdal, *Int. J. Chem. Kinet.*, 2009, **42**, 589.

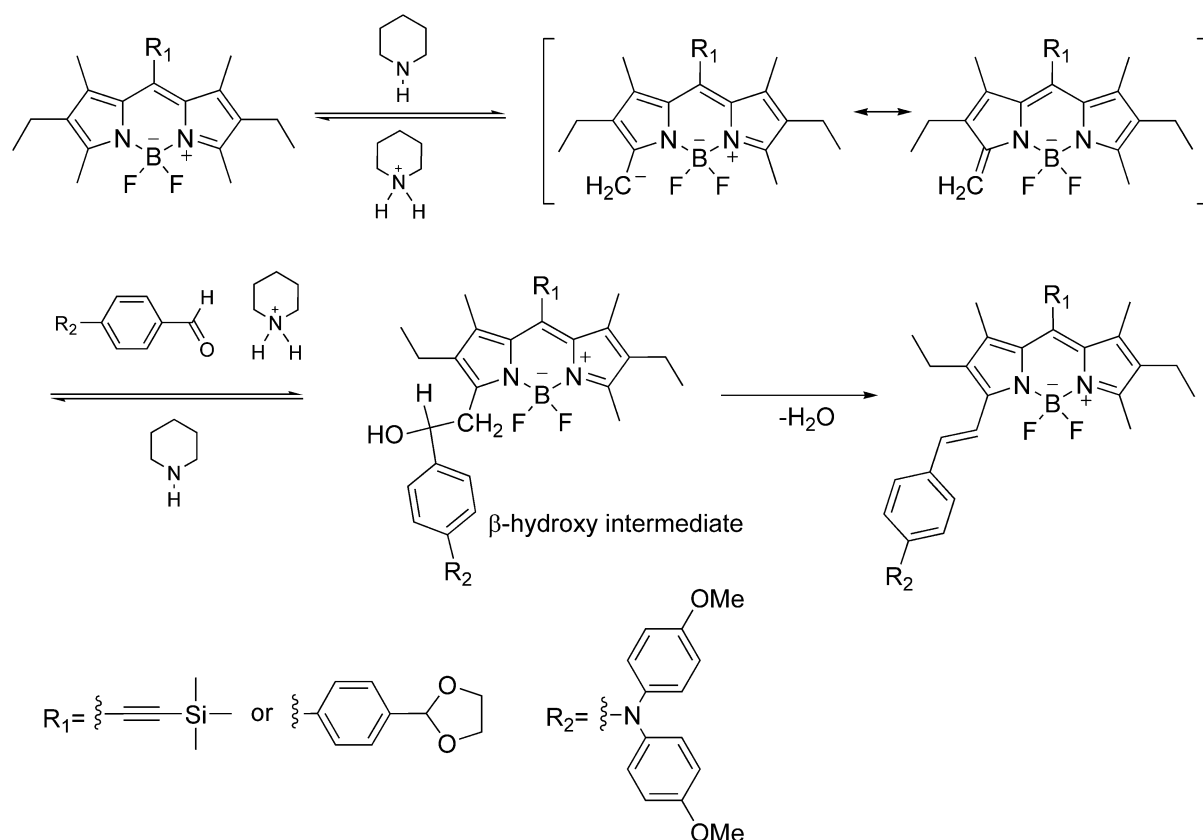


Fig. S1: Hann-Lapworth mechanism as applied to the reaction of 3,5-dimethyl-BODIPYs with aromatic aldehydes under the influence of piperidine. It is pointed out that this mechanism is only shown for a better understanding and it is **not** valid for this reaction. The validity of this mechanism was excluded by the fact the β -hydroxy intermediate was not isolated. Instead animal **B** (Fig. S2) was isolated, proving the validity of the organocatalytic mechanism show in Fig. S2.

Hence, the second mechanism, also studied by different research groups e.g. to understand the condensation between malonic acid derivatives and aromatic aldehydes in the presence of secondary amines, has to be proven for its validity regarding the reaction between BODIPYs and aromatic aldehydes.² This mechanism based on an organocatalytic way of condensing a methyl/methylene compound with an aldehyde in the presence of primary or secondary amines (Fig. S2). Here, the amine (in our case piperidine) acts primarily as a nucleophile. The proposed reaction sequences modified and adapted from ref. 2 as applied to the condensation reaction between an aromatic aldehyde and a BODIPY compound in the presence of piperidine/glacial acetic acid is shown in Fig. S2. In the first step, the amine is supposed to react with the electropositive carbonyl carbon of the aromatic aldehyde forming the hemiaminal **A** which can undergo a second nucleophilic reaction with an additional amine to form the aminal **B** under condensation. On the one hand, one piperidine molecule can be eliminated from **B** under acidic condition (to form an iminium ion **C**) on the other hand, **B** can

directly react with the methyl groups of the BODIPY compound under splitting off one piperidine molecule creating the β -amino intermediate **D**. We assume that the formation of **D** is facilitated by the basic character of piperidine. In the last step one more piperidine molecule is split off and the mono-substituted product **E** is released and can participate in a new catalysis cycle. The fact that this condensation always results in the formation of exclusively *trans*-substituted BODIPYs can be understood from the mechanism (see $^1\text{H-NMR}$ spectra of **8** and **16**, Fig. S4 and S5, showing typical *trans* coupling constants of 16.6 and 16.4 Hz, respectively). The intermediate **D** is supposed to be preferably formed in such a configuration that the steric demanding groups (donor group and BODIPY) are oriented antiperiplanar to each other. During the elimination of piperidine the *trans*-orientation is sustained. Further, it is known that the deamination step of **D** is rate determining and can be accelerated in the presence of protons. This explains the importance of the commonly added acid (glacial acetic acid or *p*-toluenesulfonic acid). The isolation of the aminal **B** (Fig. S3) proves the validity of the organocatalytic mechanism for the reaction between 3,5-dimethyl BODIPYs and aromatic aldehydes in the presence of piperidine.

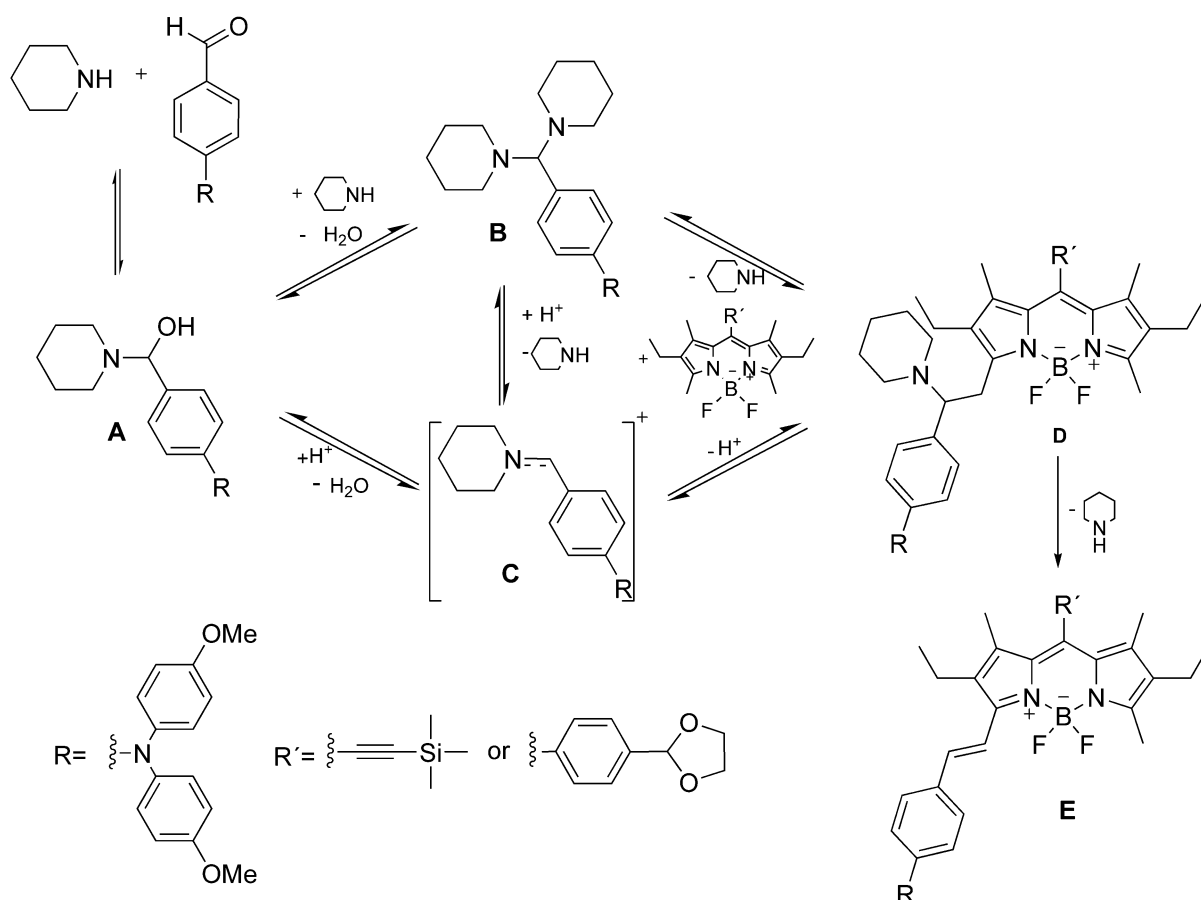


Fig. S2: Proposed mechanism for the Knoevenagel-type condensation of 3,5-dimethyl BODIPYs with aromatic aldehydes catalysed by piperidine in a non-polar aprotic solvent (modified in accordance with ref. 2).

2. NMR Spectra

General. ^1H -NMR spectra were recorded on a Bruker Avance 300 spectrometer at a transmitter frequency of 300.13 MHz. The ^1H - ^{13}C coupled NMR spectrum was recorded at a frequency of 125 MHz.

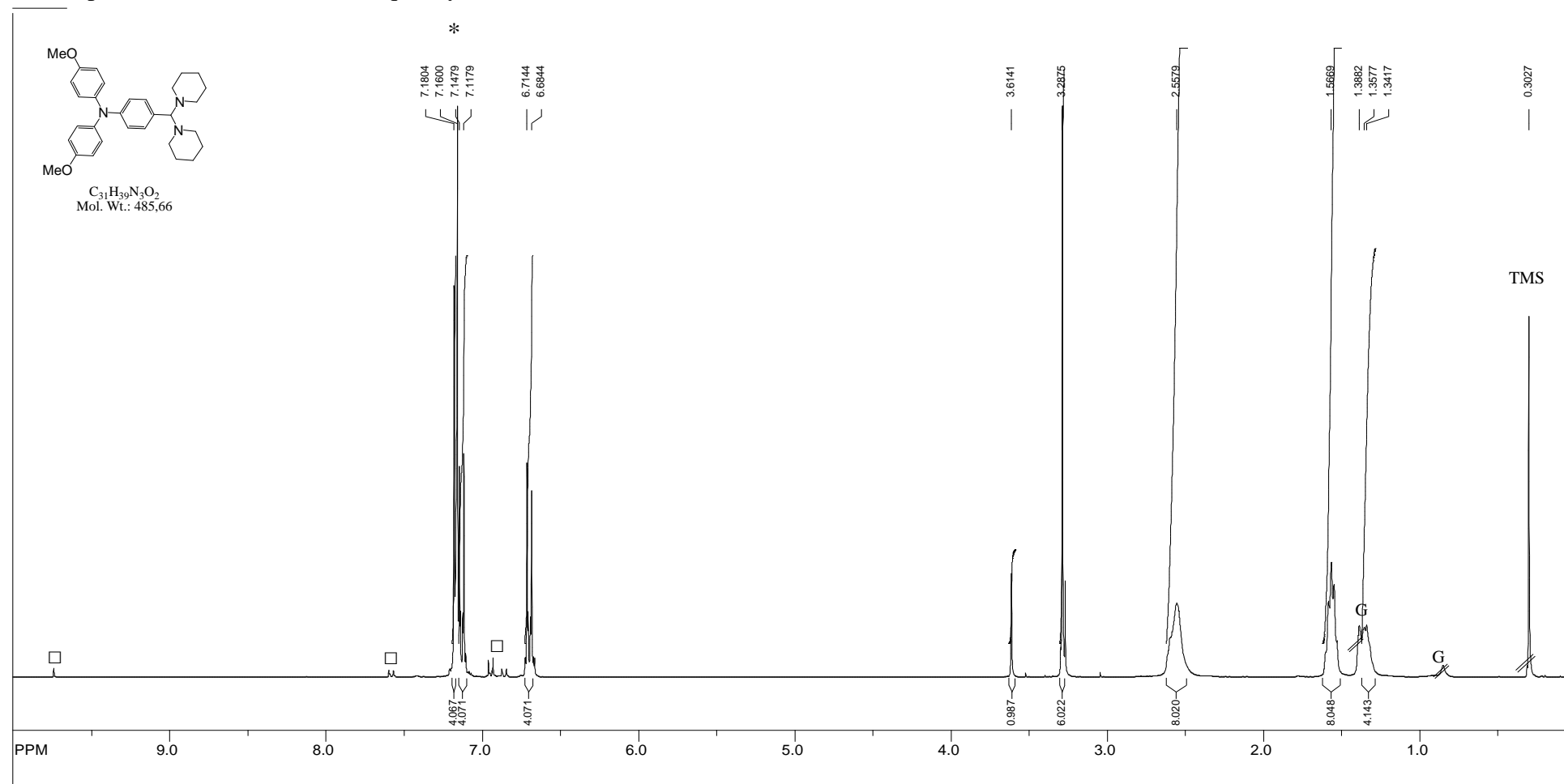


Fig. S3: ^1H -NMR spectrum of the aminal formed by the reaction of 4-(di(4-methoxyphenyl)amino)benzaldehyde and piperidine measured in C_6D_6 . (*: solvent residual signal; TMS: internal standard = tetramethylsilane; □: 4-(di(4-methoxyphenyl)amino)benzaldehyde resonance signals; G: H-grease)

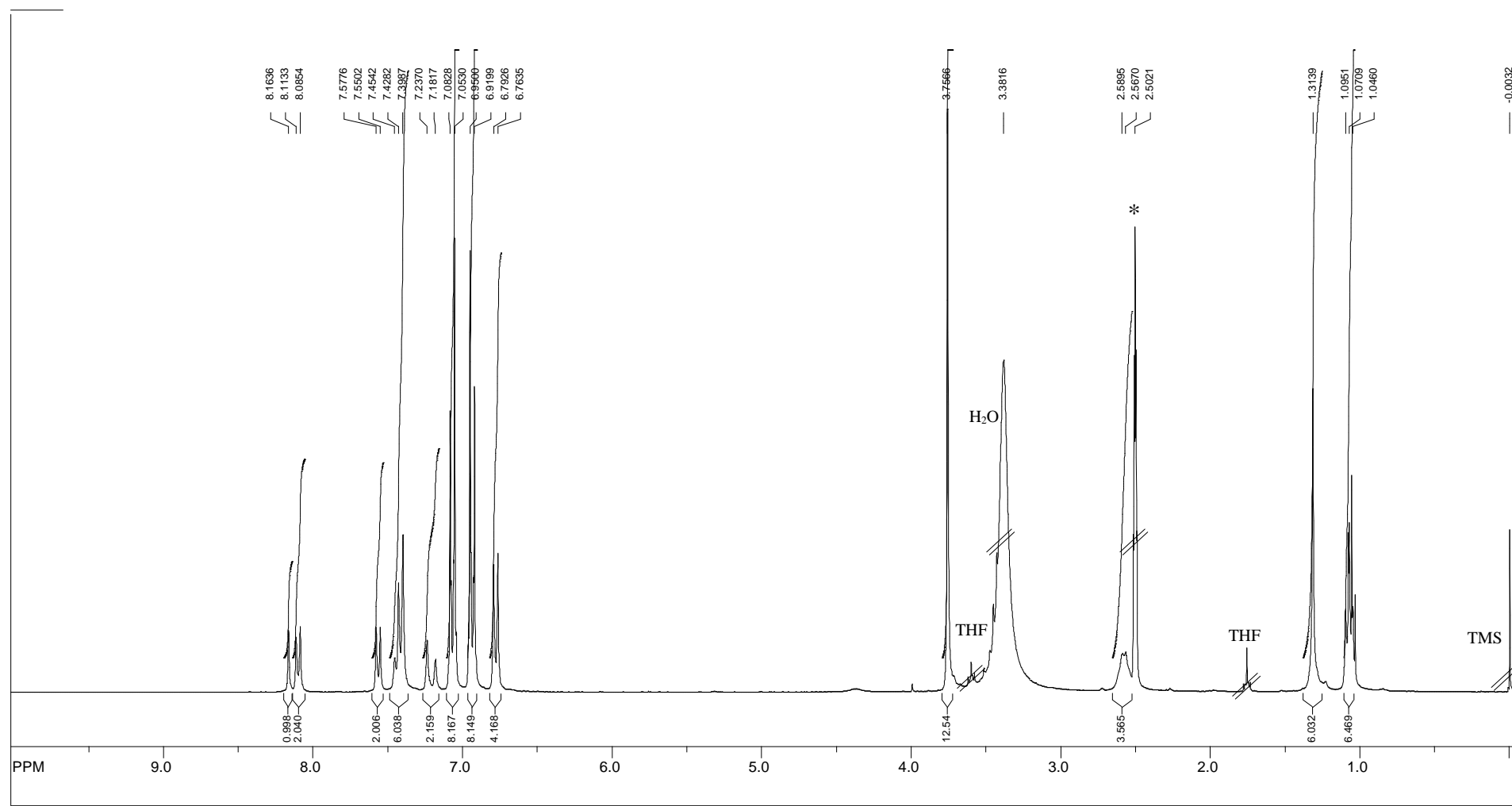


Fig. S4: ¹H-NMR spectrum of compound **8** in DMSO-d₆. (*: solvent residual signal; TMS: internal standard = tetramethylsilane; THF: tetrahydrofuran)

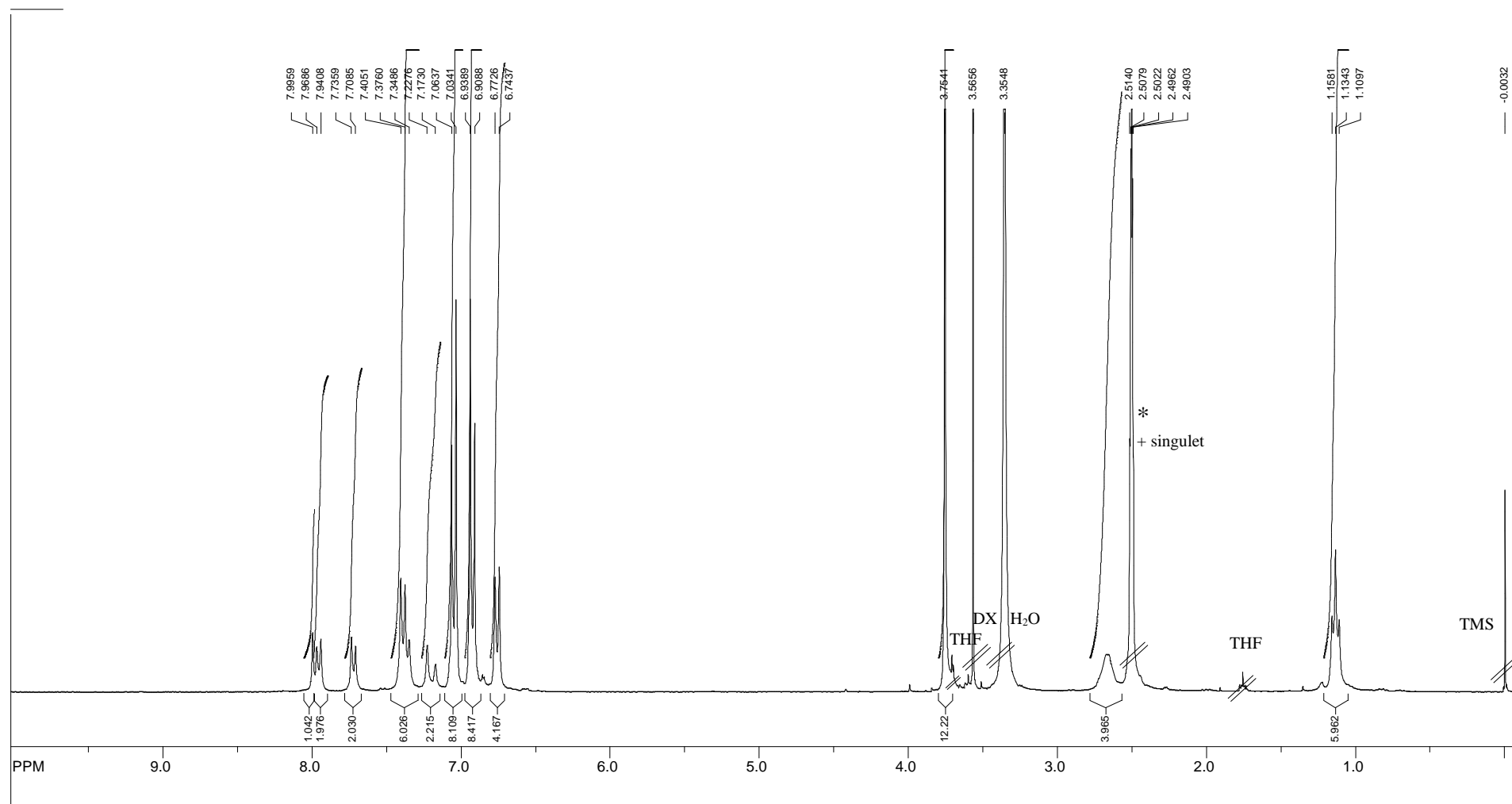


Fig. S5: ¹H-NMR spectrum of compound **16** in DMSO-d₆. (*: solvent residual signal; TMS: internal standard = tetramethylsilane; THF: tetrahydrofuran; DX: 1,4-dioxane used for freeze-drying)

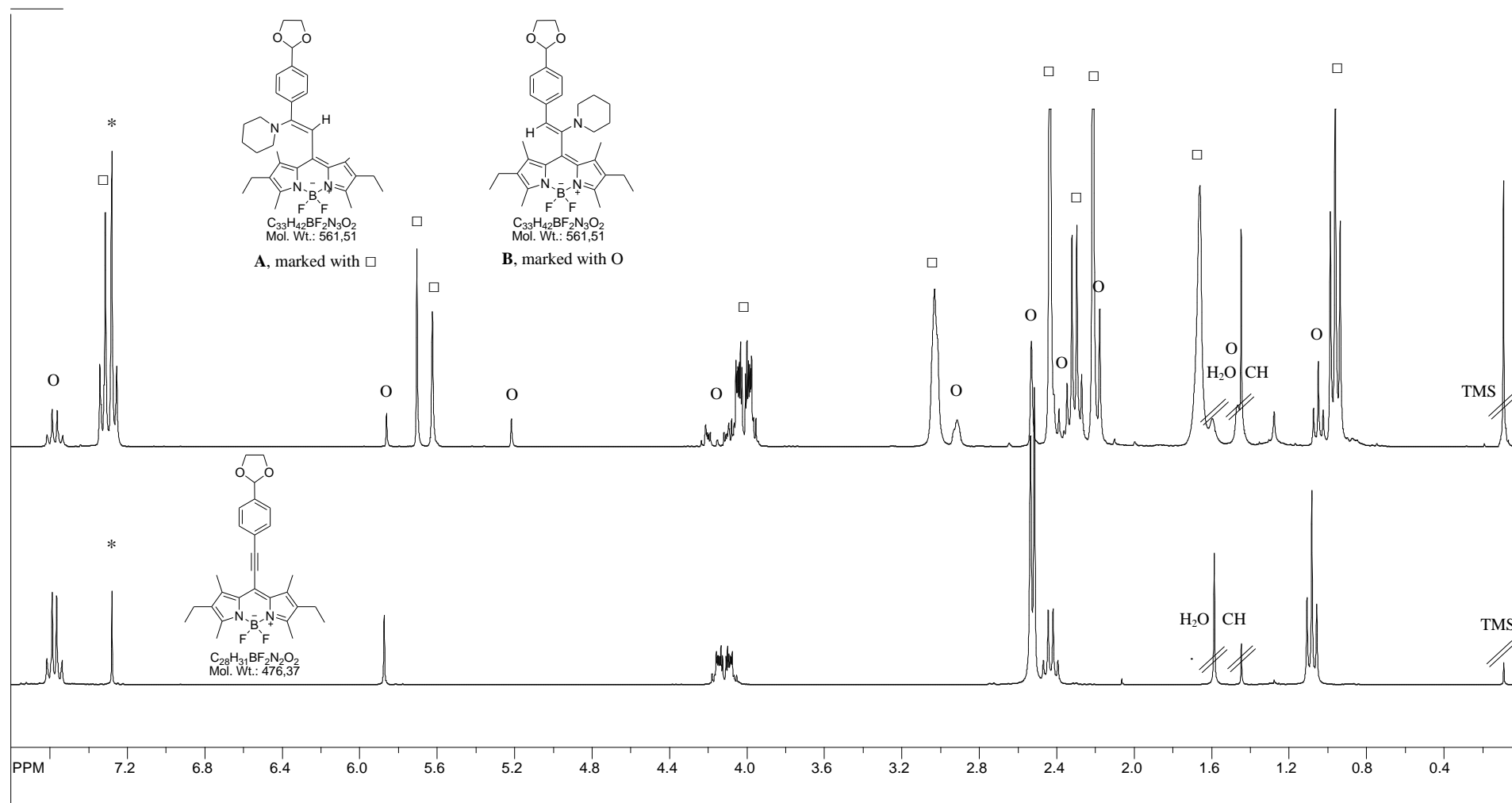


Fig. S6: ¹H-NMR spectrum of **17** (bottom) and the hydroamination products **A** and **B** (top) formed by the reaction between **17** and piperidine. (*: solvent residual signal; TMS: internal standard = tetramethylsilane; CH: cyclohexane)

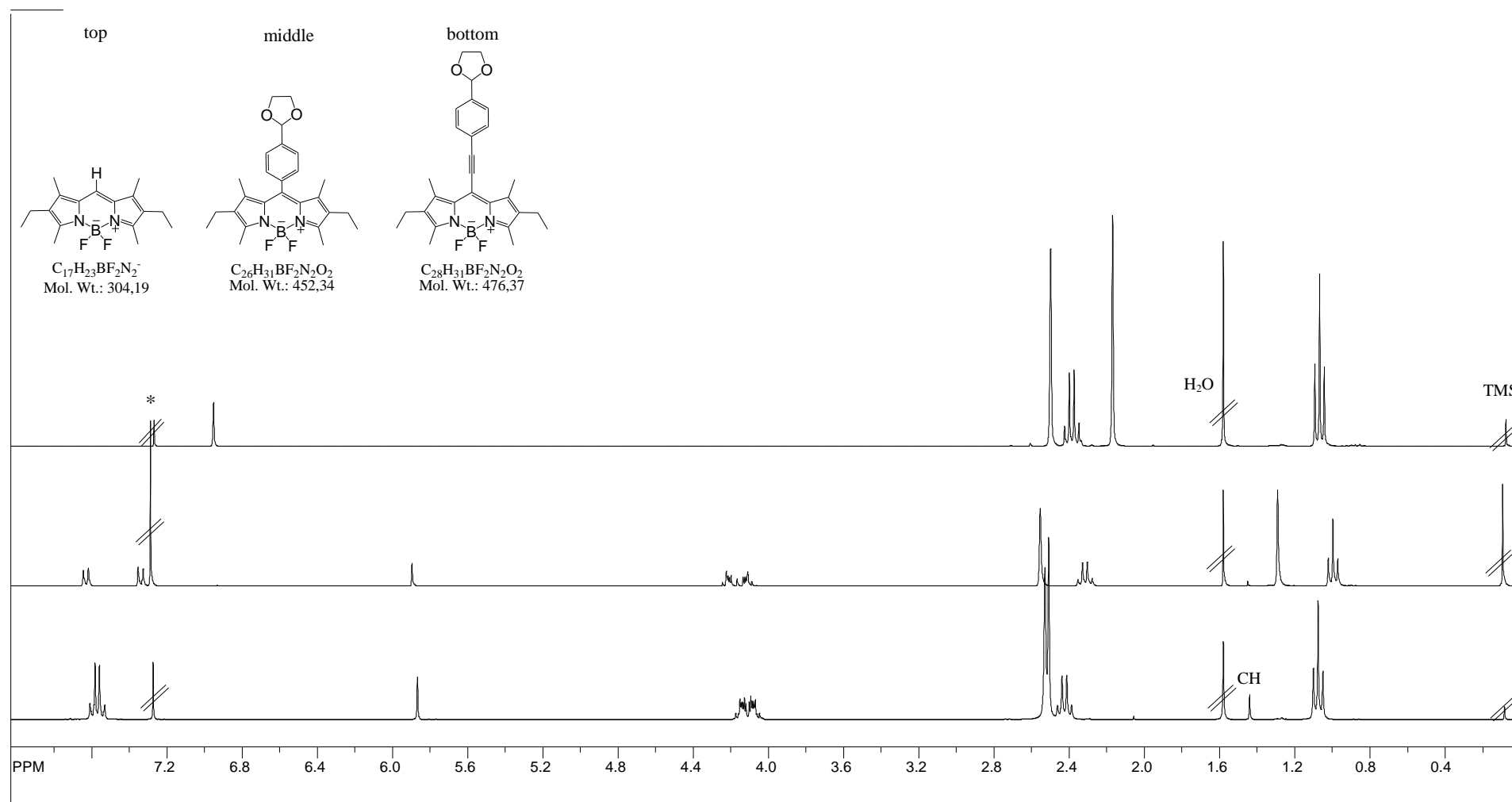


Fig. S7: ¹H-NMR spectra of the *meso*-proton BODIPY **18** (top), the corresponding *meso*-phenyl BODIPY **3** (middle) and the *meso*-ethynylphenyl BODIPY **17** (bottom). (*: solvent residual signal; TMS: internal standard = tetramethylsilane; CH: cyclohexane)

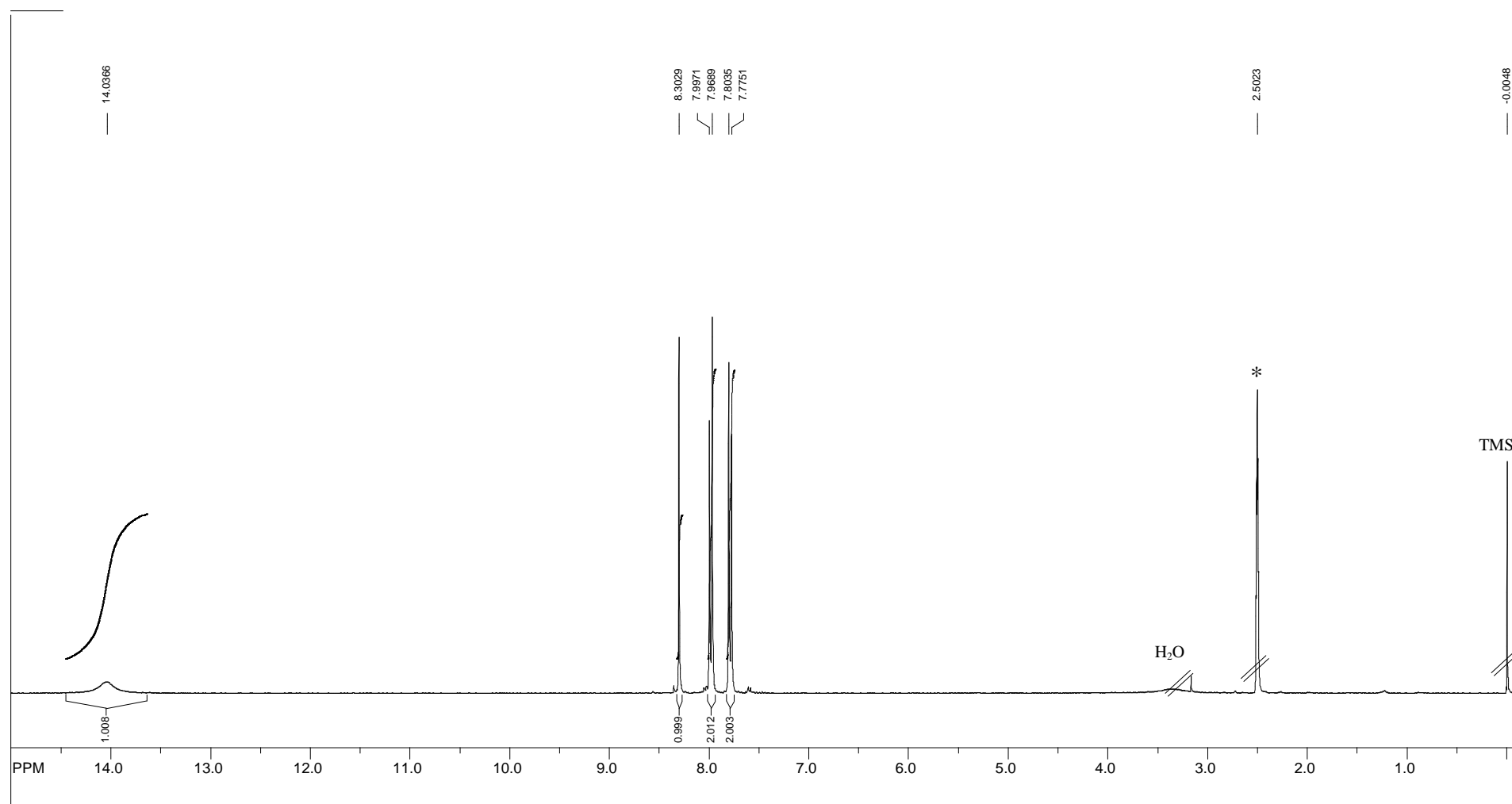


Fig. S8: ¹H-NMR spectrum of compound **12** in DMSO-d₆. (*: solvent residual signal; TMS: internal standard = tetramethylsilane)

3. Determination of the double bond geometry of **12**

Unfortunately, for trisubstituted olefins this information cannot be deduced from the $^1\text{H-NMR}$ spectrum because there are no vicinal protons. In general, the configuration of such alkenes can be determined by measuring the nuclear Overhauser effect (NOE) and by performing proton coupled or gated decoupling NMR experiments. In our case, the measurement of the NOE could not be used for the determination of the configuration because the resonance signal of the proton of the carboxylic group is extremely broad in the $^1\text{H-NMR}$ spectrum (Fig. S8). This indicates a very short relaxation time for this proton. Additionally, it is known that the NOE build-up time is very slow for small molecules. Hence, even if the carboxyl group would come close to the aromatic proton (*cis* configuration) no NOE would be measurable. Thus, we performed a proton coupled $^{13}\text{C-NMR}$ experiment on **12** (Fig. S9). The spectrum shows the resonance signals for of the ten C-atoms and their splitting due to $^1J_{\text{C/H}}$, $^2J_{\text{C/H}}$ and $^3J_{\text{C/H}}$ couplings. Of special interest are signal *a* with a vicinal $^3J_{\text{C/H}}$ coupling constant of 6.7 Hz and signal *f* with vicinal $^3J_{\text{C/H}}$ coupling constant of 13.9 Hz arising from the carbon atoms of the COOH and CN group, respectively. It is known from the literature that *cis*-vicinal $^3J_{\text{C/H}}$ coupling constants of substituted alkenes are usually smaller than comparable *trans*-vicinal $^3J_{\text{C/H}}$ coupling constants.³

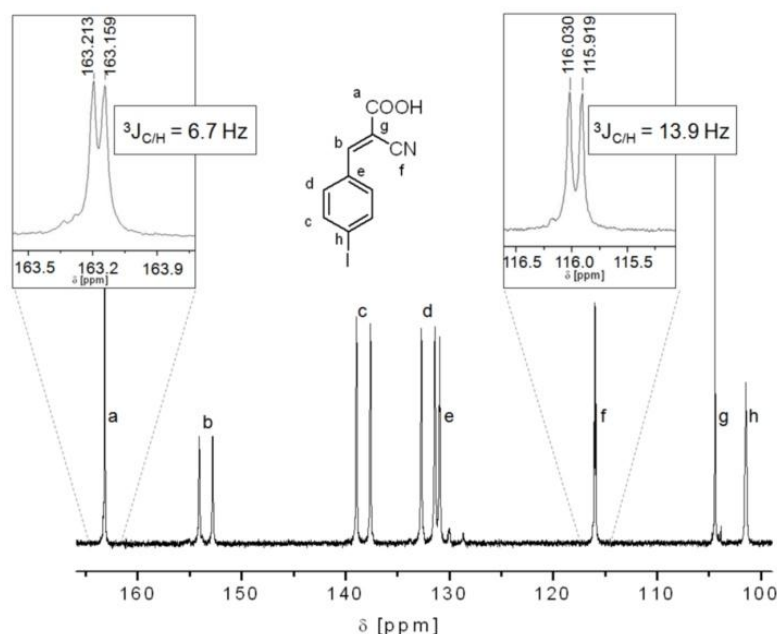


Fig. S9: Proton coupled $^{13}\text{C-NMR}$ of **12**. The spectrum shows the ^{13}C resonance signals and their splitting due to the $^1J_{\text{C/H}}$, $^2J_{\text{C/H}}$ and $^3J_{\text{C/H}}$ couplings. The insets show the splitting of the resonance signals arising from the COOH group (a) and the CN group (f).

³ U. Vogeli and W. von Philipsborn, *Org. Magn. Reson.*, 1975, **7**, 617

4. UV/vis Spectra

General. UV/vis spectra were recorded in CH₂Cl₂ on a Hitachi U-3000 spectrophotometer at a concentration in the range of 1·10⁻⁵ M.

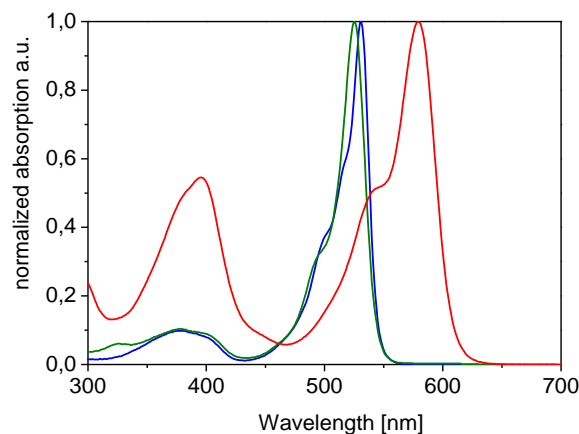


Fig. S10: UV/vis spectra of **18** (blue), **3** (olive) and **17** (red).

5. Cyclic Voltammetry Data

General. Cyclic voltammetry (CV) was carried out under moisture- and oxygen-free conditions using a standard three-electrode assembly connected to a potentiostat (model 263A, EG&G Princeton Applied Research) at a scanning rate of 50 mV sec⁻¹. A Pt milli-electrode (model G0228, AMETEK Advanced Measurement Technology) was used as working electrode. A platinum wire in the respective solvent plus conducting salt (tetrabutylammonium hexafluorophosphate, 0.1 M) was used as counter electrode and the quasi-reference electrode consisted of an Ag-wire in an AgNO₃/acetonitrile solution (0.1 M). Each measurement was calibrated with the internal standard ferrocene/ferrocenium. The energy levels were determined by the empirical relation:

$$E^{\text{HOMO or LUMO}} = [-e \cdot (E^{1/2}_{(x \text{ vs. Ag/AgNO}_3)} - E^{1/2}_{(\text{Fc/Fc}^+ \text{ vs. Ag/AgNO}_3)})] - 4.80 \text{ eV}.$$
$$(E^{1/2}_{(\text{Fc/Fc}^+ \text{ vs. Ag/AgNO}_3)} = 0.13 \text{ eV})$$

Due to the fact that on attaching the cyanocarboxylic acid anchoring group the anodic and cathodic peak currents decrease in compounds **5**, **8**, **13** and **16**, the cyclic voltammograms of the corresponding deprotected BODIPYs (**4**, **7**, **11**, **15**) are depicted, as well.

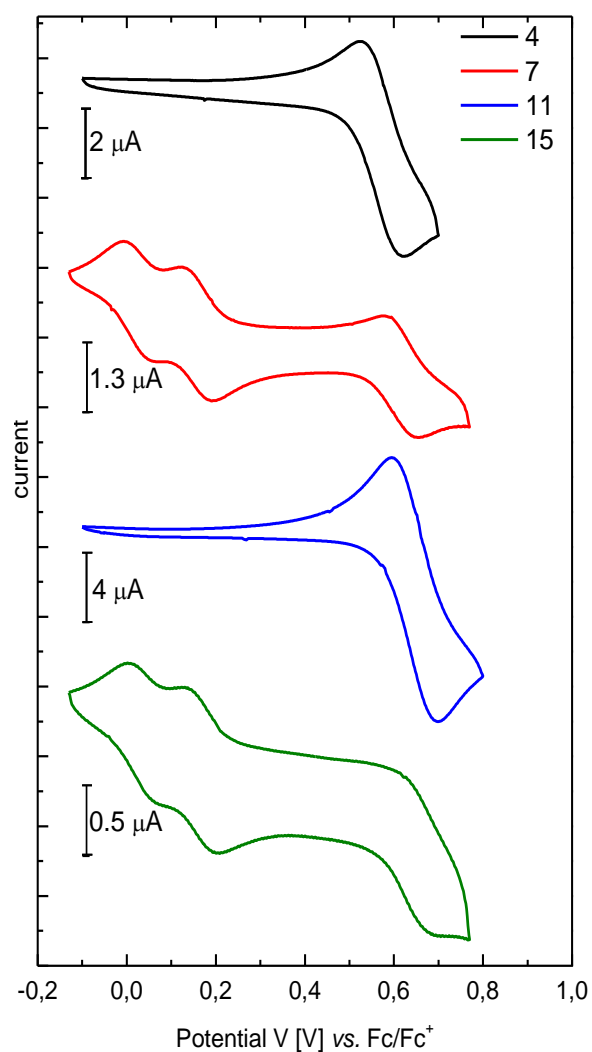


Fig. S11: CV-curves for the energy level determination of **4**, **7**, **11** and **15**.

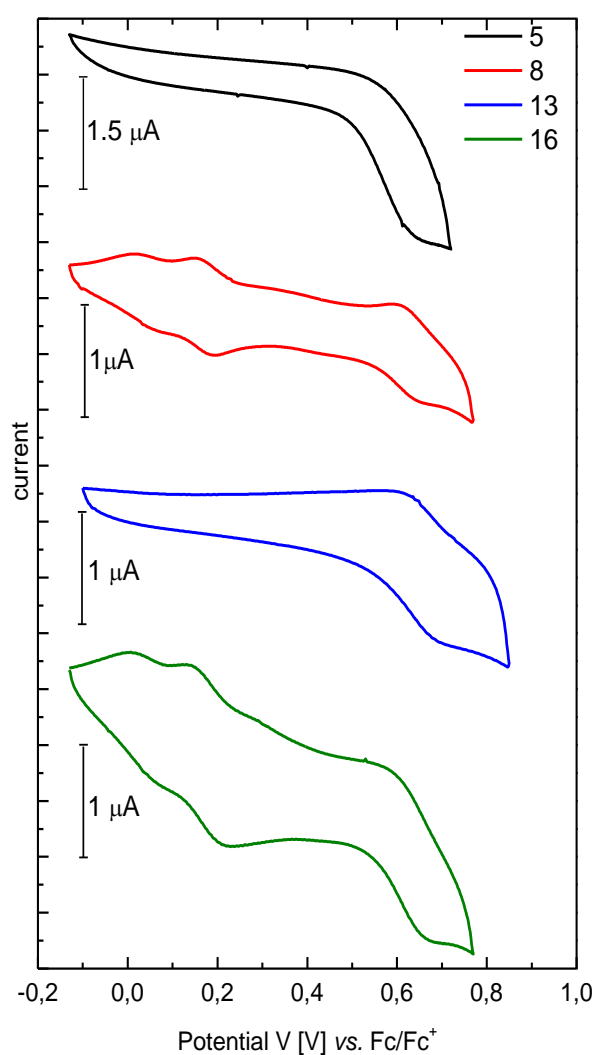
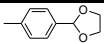
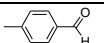
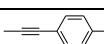
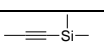
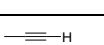
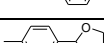
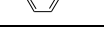
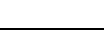


Fig. S12: CV-curve for the energy level determination of **5**, **8**, **13** and **16**.

Table S1: Summary of the measured and the calculated energy levels on the basis of cyclic voltammetry experiments carried out at 50 mV/sec in CH₂Cl₂ with 0.1 M tetrabutylammonium hexafluorophosphate using ferrocene as reference.

compd	E ^{1/2} _{OX1} [V]	E _{OX1} [eV]	E ^{1/2} _{OX2} [V]	E _{OX2} [eV]	E ^{1/2} _{OX3} [V]	E _{OX3} [eV]	E ^{1/2} _{RED} [V]	E _{RED} [eV]	E _{LUMO} ^{a)} [eV]	R in pos. 8	R in pos. 3 and 5
3	0.60	-5.40	---	---	---	---	-1.68	-3.12	-3.12		CH ₃
4	0.58	-5.38	---	---	---	---	-1.65	-3.15	-3.12		CH ₃
5	0.60	-5.40	---	---	---	---	---	---	-3.18		CH ₃
17	0.63	-5.43	---	---	---	---	---	---	-3.39		CH ₃
10	0.62	-5.42	---	---	---	---	-1.45	-3.35	-3.34		CH ₃
11	0.64	-5.44	---	---	---	---	---	---	-3.36		CH ₃
13	0.64	-5.44	---	---	---	---	---	---	-3.48		CH ₃
6	0.02	-4.82	0.16	-4.96	0.60	-5.40	-1.56	-3.24	-3.23		= - DiOMeTPA ^{b)}
7	0.03	-4.83	0.16	-4.96	0.62	-5.42	---	---	-3.26		= - DiOMeTPA ^{b)}
8	0.04	-4.84	0.17	-4.97	0.62	-5.42	-1.53	-3.27	-3.28		= - DiOMeTPA ^{b)}
15	0.04	-4.84	0.17	-4.97	0.65	-5.45	---	---	-3.40		= - DiOMeTPA ^{b)}
16	0.04	-4.84	0.18	-4.98	0.63	-5.43	---	---	-3.59		= - DiOMeTPA ^{b)}

^{a)} The LUMO level was calculated from the optical band gap. ^{b)} 4,4'-dimethoxytriphenylamine.

Note: **14** could not be measured because the protection group was removed by the conducting salt very fast. In contrast to that, the deprotection of **10** proceeded more slowly.